Polyconjugated Azomethine Layers by Sequential Condensation of α,α′-Dialdehyde-oligothiophenes and 4,4′-Diamino-diphenylenes on ITO/Glass Electrodes

Gianni Zotti* and Albarosa Randi

Istituto CNR per l' Energetica e le Interfasi, C.o Stati Uniti 4, 35127 Padova, Italy

Silvia Destri and William Porzio

Istituto CNR per lo Studio delle Macromolecole, via E. Bassini 15, 20133 Milan, Italy

Giovanni Schiavon

Istituto CNR di Chimica Inorganica e delle Superfici, C.o Stati Uniti 4, 35127 Padova, Italy

Received June 5, 2002. Revised Manuscript Received September 12, 2002

Sequential (alternate) azomethine condensation of aldehyde end-capped oligothiophenes (Tn, $n = 3$, 6, and 8) with *p*-diaminobiphenile (DAB) or *p*-diaminofluorene (DAF) on 3-aminopropyltrimethoxysilane-primed (ATS-primed) ITO/glass is reported. The layers have been characterized by cyclic voltammetry, UV−vis spectroscopy, photoluminescence, XRD, and AFM. The oligothiophene layers first produced on the ATS-primed ITO are dense like ferrocene monolayers for T3 (4×10^{-10} mol cm^{-2}) and ca. 3 times less dense for T6 and T8 (1.5×10^{-10} mol cm^{-2}). The subsequent sequential growth occurs regularly with T3 but its rate is ca. 50% lower for T6 and almost null for T8. The condensed films are free of major defects and have the same roughness as the primed surface. Typical brush-electrodes formed by ATS/T3/$(DAF/T3)_4$ and ATS/T6/$(DAF/T6)_2$ sequences are fluorescent and reversibly protonated to colored films by perchloric acid in acetonitrile and undergo reversible iodine-doping.

1. Introduction

A challenge in material science is the creation of supramolecular materials in which the constituent units are highly ordered macromolecules. In a bottom-up approach, larger entities, i.e., quasi crystalline layers, can be formed by spontaneous assembly of molecules. The key point to build up these arrangements is how the smaller units self-organize on surfaces. There are many examples of organosulfur compounds regularly assembled on gold to generate ordered structures[1,2] or of organosilicon derivatives forming layers on glass, quartz, mica, and silicon oxide.[2] As a particular example, a layer-by-layer self-assembled organosilicon derivative on indium−tin-oxide (ITO), showing a large electrooptical response, has been recently presented by Marks.[3] Also, block copolymers form regular structures on glass, due to repulsive and attractive forces among the intrinsically different segments and among themselves and the substrate.[4] However, quite often, preformed polymers are cast or spun on the surface instead of growing the chains layer-by-layer normally to the substrate. The former procedure has been employed for polyazomethines,[5a,b] polyquinoxalines,[6] and polyamides[7] using high-vacuum deposition. For polyazomethines the sequential growth was also used. In this regard, a recent report[8] presented some oligoazomethine phenylene monolayers for the production and the investigation of model molecular wires.[9,10]

Aromatic polyazomethines constitute a known class of polyconjugated polymers which has recently gained a noticeable interest in the field of nonlinear optical devices.[11] Polymers containing *p*-phenylene or *p*-diphenylene aromatic moieties were synthesized by condensation polymerization of diamines and dialdehydes or diketones.[12,13]

* To whom correspondence should be addressed. Tel (39) 049-829-5868; fax (39) 049-829-5853; e-mail gzotti@ipelp.pd.cnr.it.

(1) Poirier, G. E. *Chem. Rev.* **1997**, *97*, 1117.
(2) Ulman, A. *Chem. Rev.* **1996**, *96*, 1533.
(3) Van der Boom, M. E.; Richter, A. G.; Malinsky, J. E.; Lee, P. A.; Armstrong, N. R.; Dutta, P.; Marks, T. J. *Chem. Mater.* **2001**, *13*, 15.
(4) Stocker, W.; Beckmann, J.; Stadler, R.; Rabe, J. P. *Macromolecules* **1996**, *80*, 2224.
(5) (a) Weaver, M. S.; Bradley, D. D. C. *Synth. Met.* **1996**, *83*, 61. (b) Fischer, W.; Stelzer, F.; Meghdadi, F.; Lleising, G.; *Synth. Met.* **1996**, *76*, 201.
(6) Alvarado, S. F.; Reiss, W.; Jandke, M.; Strohrielg, P. *Org. El.* **2001**, *2*, *75*.
(7) Muguruma, H.; Yudasaka, M.; Hotta, S. *Thin Solid Films* **1999**, *339*, 120.
(8) Rosink, J. J. W. M.; Blaw, M. A.; Geeligs, L. J.; Van der Drift, E.; Rousseeuw, B. A. C.; Radelaar, S. *Langmuir* **2000**, *16*, 4547.
(9) Onipko, A. I.; Berggren, K. F.; Klymenko, Y. O.; Malysheva, L. I.; Rosink, J. J. W. M.; Geerligs, L. J.; Van der Drift, E.; Radelaar, S. *Phys. Rev. B.* **2000**, *61*, 11118.
(10) Rosink, J. J. W. M.; Blauw, M. A.; Geerligs, L. J.; Van der Drift, E.; Radelaar, S. *Phys. Rev. B.* **2000**, *62*, 10459.
(11) Amari, C.; Pelizzi, C. Predieri, G.; Destri, S.; Porzio, W.; Einseidel, H. Menges, B.; Mittler-Neher, S. *J. Mater. Chem.* **1996**, *6*, 1319.

10.1021/cm020619v CCC: $22.00
Published on Web 10/22/2002

Chart 1

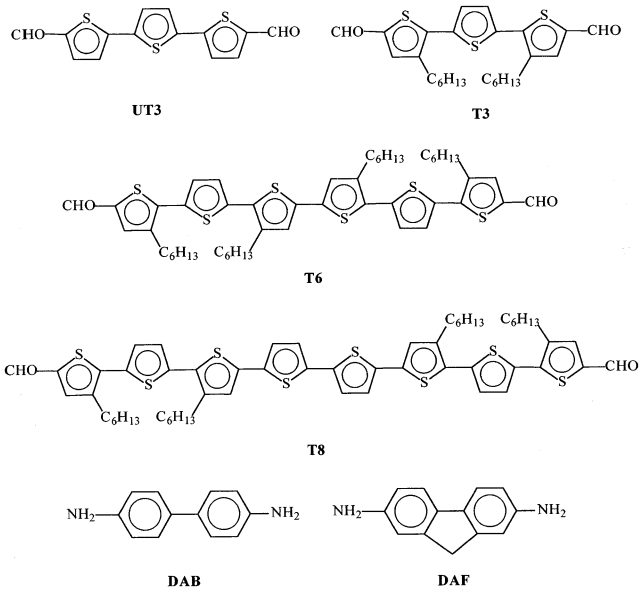

Sequential aromatic polyazomethines might be interesting materials for the construction of superlattices which can find employment in data networking and telecommunication, particularly if they are produced on proper surfaces. Following these ideas, the α,α′-aldehyde-bifunctionalized oligothiophenes shown in Chart 1 were used in alternation with *p*-diaminobiphenyle (DAB) or *p*-diaminofluorene (DAF) for the fabrication of π-conjugated azomethine oligomer chains attached to the surface, as exemplified in Scheme 1. We previously reported the formation of polyazomethine polymers from these monomers and DAB.[14,15] In this paper we extended this polymerization to an electrode (ITO/glass) surface in order to produce electrically addressed and (possibly) ordered oligomer strands (brush-electrodes). Characterization of the resulting brush-electrodes was performed with cyclic voltammetry, UV−vis spectroscopy, photoluminescence, X-ray diffraction, and atomic force microscopy.

2. Experimental Section

2.1. Chemicals, Materials, and Reagents. Acetonitrile was reagent grade (Uvasol, Merck) with a water content of <0.01%. The supporting electrolyte tetrabutylammonium perchlorate (Bu_4NClO_4) was previously dried under vacuum at 70 °C.

The thiophene oligomers 5,5″-dicarboxyaldehyde-3,3″-dihexyl-2,2′:5′,2″-terthiophene (T3), 5,5⁗-dicarboxyaldehyde-3,3‴,3⁗-tetrahexyl-2,2′:5′,2″:5″,2‴:5‴,2⁗:5⁗,2⁗⁗-sexithiophene (T6), 5,5⁗⁗-dicarboxyaldehyde-3,3″,3⁗,3⁗⁗-tetrahexyl-2,2′:5′,2″:5″,2‴:5‴,2⁗:5⁗,2⁗⁗:5⁗⁗,2⁗⁗⁗-octathiophene (T8),[16] and 5,5″-dicarboxyaldehyde-2,2′:5′,2″-terthiophene (UT3)[17] (Chart 1) were prepared according to the literature. 2,7-Diamino fluorene (DAF) and 4,4′-diamino-1,1′-biphenyle (DAB) were purchased from Aldrich, and 3-aminopropyltrimethoxysilane (ATS) was purchased from Fluka.

ITO/glass electrodes were 1 × 4 cm indium−tin-oxide one-side-coated glass sheets (20 ohm sq^{-1}, Balzers, Liechtenstein). The ITO/glass microstructure consists of grains ca. 100 nm long and ca. 15 nm high with an amorphous phase along the grain boundaries.

2.2. Procedure for the Sequential Condensation. The ITO/glass electrodes were cleaned with acetone and dried prior to use. Sequential condensation was performed on both the ITO and the glass surfaces of the ITO/glass electrode after surface silanization with ATS performed according to the literature.[18] Briefly, the clean ITO/glass substrate was immersed for 1 h in 5% ATS solution in nitrogen-degassed dry toluene and then washed with dry toluene and dried.

A sequential (alternate) condensation of a dialdehyde (terephthal-dicarboxaldehyde) and a diamine (4,4′-diamino-phenylene) was reported only a short time ago.[8] The process, based on reaction from solution, is so slow that it requires days (24 h per step). In our case the condensation is sped up by performing it at a temperature close to the melting point of the compound.

The same procedure was used for each component and consisted of (1) dipping the sample for 5 min in the appropriate monomer solution; (2) curing the wet sample at 120 °C for 15 min; (3) washing the sample carefully in the solvent used for monomer casting (to eliminate monomer excess); and (4) drying. DAF and DAB were used in 10^{-3} M concentration in acetonitrile whereas the oligothiophenes were used either in acetonitrile solution for the most soluble terthiophenes (5×10^{-4} M for UT3 and 1×10^{-3} M for T3) or $CHCl_3$ solution for the higher oligothiophenes (5×10^{-4} M for T6 and 1×10^{-4} M for T8).

The curing (condensation) (step 2) was cautiously performed under vacuum for safety reasons (due to the toxicity of aromatic diamines) and to avoid any possible aerial decomposition. However, the small amount of the toxic starting compounds allowed us to check that performing the reaction in air caused neither any significant degradation of the materials nor differences in the formed layers. Longer reaction times, e.g., 30 min dipping and 60 min curing, did not increase the reaction conversion.

The sequential build-up was monitored by CV and UV−vis spectroscopy. For the latter the absorbance data are given as measured, i.e., for the sum of the ITO and glass sides. As a confirmation that the oligomer forms up to the same level at both sides of the electrode, electrochemical overoxidation of the modified electrode at 2 V followed by reduction at −2 V, which bleaches the material, causes a 50% decrease of the absorbance.

All the available surface sites are involved in the one-step condensation reaction as the repetition of the overall procedure leaves the previous coverage practically unchanged.

2.3. Apparatus. Electrochemical experiments were performed at room temperature under nitrogen in three electrode cells. The counter electrode was platinum; reference electrode was a silver/0.1 M silver perchlorate in acetonitrile (0.34 V vs SCE). The voltammetric apparatus (AMEL, Italy) included a 551 potentiostat modulated by a 568 programmable function generator and coupled to a 731 digital integrator.

Electronic spectra were taken with a Perkin-Elmer Lambda 15 spectrometer.

Photoluminescence (PL) measurements were performed with a SPEX 270M polychromator equipped with a N_2-cooled CCD detector by exciting at 454 nm with a monochromated Xe-lamp.

Atomic force microscopy (AFM) measurements were performed on 1 × 1 cm glass sections mounted on ca. 1.5-cm diameter steel disks with adhesive tabs. Experiments were conducted in air at ca. 295 K using a Digital Multimode STM

(12) Park, S. B.; Kim, H.; Zin, W. C.; Jung, J. C. *Macromolecules* **1993**, *26*, 1627.
(13) Yang, C. J.; Jenekhe, S. A. *Macromolecules* **1995**, *28*, 1180.
(14) Olinga, T. E.; Destri, S.; Botta, C.; Porzio, W.; Consonni, R.; *Macromolecules* **1998**, *31*, 1070.
(15) Destri, S.; Khotina, I. A.; Porzio, W. *Macromolecules* **1998**, *31*, 1079.
(16) Olinga, T.; Destri, S.; Porzio, W.; Selva, A. *Macromol. Chem. Phys.* **1997**, *198*, 1091.
(17) Destri, S.; Dubisky, Y.; Porzio, W. *Synth. Met.* **1995**, *75*, 25.
(18) Decher, G.; Hong, J. *Makromol. Chem. Macromol. Symp* **1991**, *46*, 321; Decher, G.; Hong, J. *Ber. Bunsen-Ges. Phys. Chem* **1991**, *95*, 1430.

Scheme 1

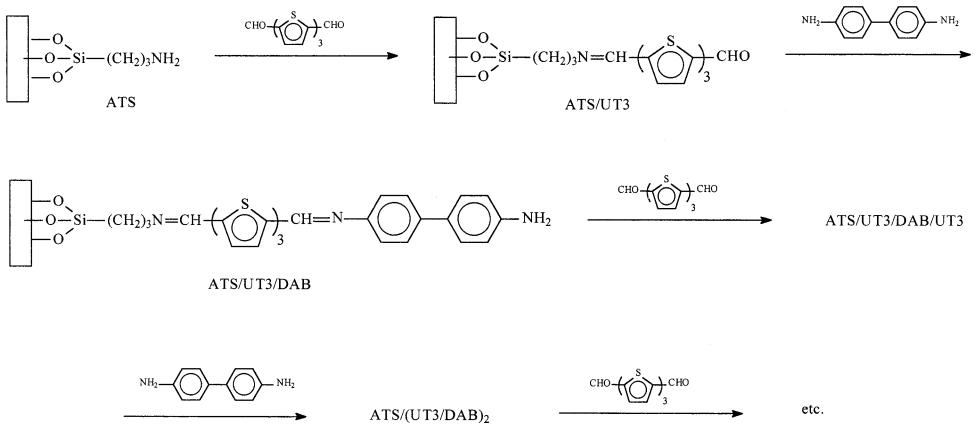

Table 1. Monomer Oxidation ($E°_{Ox}$) and Reduction Potentials ($E°_{Red}$) in Acetonitrile; Maximum Absorption (λ_{Max}) and Molar Extinction Coefficient (ϵ) in $CHCl_3$

monomer	$E°_{ox}$/V	$E°_{red}$/V	λ_{max}/nm	ϵ/M^{-1} cm^{-1}
UT3	1.06	−1.62	413	4.0×10^4
T3	1.00	−1.68	402	3.7×10^4
T6	0.60; 0.82	−1.80	443	4.0×10^4
T8	0.34; 0.60	−1.82	468	5.0×10^4
DAF	0.01; 0.33	−	296, 335	−
DAB	0.16; 0.40	−	285	−

equipped with tapping mode etched silicon tips (TESP, force or spring constant 20−100 N m^{-1}; nominal tip radius curvature 5−10 nm; cantilever length 125 μm) and "J" type scanner (x−y range 125 μm; z range 5 μm). The AFM was operated in tapping mode at scan rates from 1 to 1.5 Hz.

X-ray diffraction (XRD) experiments were performed at room temperature using a Siemens D-500 diffractometer equipped with graphite monochromator and Soller slits in Bragg−Brentano geometry.

3. Results and Discussion

3.1. Electrochemistry of Oligothiophenes and Diamines. In this section the electrochemical and optical parameters of the individual building blocks used in this investigation are reported. Redox potentials, absorption maxima, and molar extinction coefficients of the monomers are summarized in Table 1.

The cyclic voltammogram CV of the aldehyde end-capped oligothiophenes in CH_2Cl_2 + 0.1 M Bu_4NClO_4 shows a one-electron reversible oxidation process. For UT3 and T3 a moderately high scan rate (>1 V s^{-1}) is required for full reversibility, given the higher tendency toward water (as moisture) attack of the radical cation. In fact, at lower scan rates the process becomes irreversible and involves 2 F mol^{-1}. Oligomers T6 and T8 display a further reversible one-electron oxidation process at higher potentials.

A two-electron reduction process is shown for all the oligothiophenes. The peak potential separation is ca. 80 mV, indicating only a small difference between the redox potentials for the two subsequent one-electron reduction processes. Therefore the $E°$ value of the overall process may be taken in practice as that of the first reduction process.

The diamines are reversibly oxidized in two one-electron reversible steps according to a well-known behavior.[19] Given their low oxidation potential and high optical energy gap their reduction potential is not accessible under our conditions.

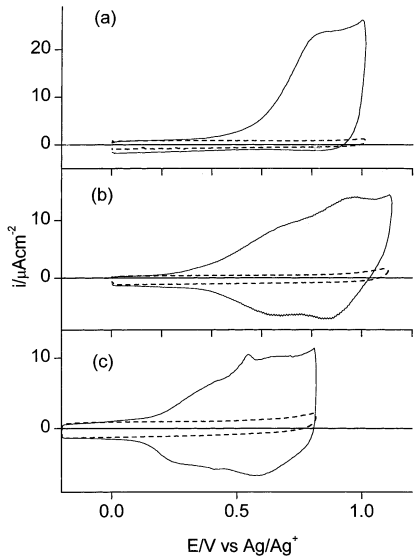

Figure 1. Cyclic voltammograms of (a) ATS/T3, (b) ATS/T6, and (c) ATS/T8 layers in acetonitrile + 0.1 M Bu_4NClO_4. Scan rate: 0.1 Vs^{-1}.

3.2. Condensation of Oligothiophene Dialdehydes on ATS-Primed ITO/Glass. The condensation of T3 to the ATS-primed ITO/glass is evidenced by CV in acetonitrile + 0.1 M Bu_4NClO_4 showing an irreversible oxidation process as a broad response at E_p = 0.80 V (Figure 1a). The charge therein involved is ca. 90 μC cm^{-2}, and because the process involves 2 electrons per molecule the response is compatible with a full monolayer coverage (45 μC cm^{-2}, i.e., 4.6×10^{-10} mol·cm^{-2}, for ferrocene[20]).

A theoretical evaluation of coverage degree was performed by molecular mechanics calculations using the MATSTUDIO program.[21] As an example, a molecular area of ca. 35 $Å^2$ was derived for T3 as the molecular axis is tilted from the substrate normal by ca. 25°. From this value it is possible to calculate the maximum number of molecules per cm^2 ($\sim 2.8 \times 10^{18}$) comparable with the value obtained by the CV coulometric data (2.4×10^{18}), confirming an almost complete coverage.

(19) Stechan, E. In *Organic Electrochemistry*; Lund, H., Baizer, M. M., Eds.; Dekker: New York, 1991; p 581.
(20) Gui, J. Y.; Stern, D. A.; Lu, F.; Hubbard, A. T. *J. Electroanal. Chem.* **1991**, *305*, 37.
(21) Materials Studio, Release 2.0, Accelrys, Parc Club Orsay Universitè 20, Rue Jean Rostand, 91898 Orsay Cedex France.

The UV−vis spectrum of the T3-layered electrode shows a maximum absorption centered at 400 nm (the same value observed for the compound in solution) and with an absorbance of 25×10^{-3}. An evaluation of the absorption cross-section of the compounds is necessary to address the coverage degree. In fact, the comparison between the value of 1.41 Å^2,[22] derived considering the extinction coefficient of T3 reported in Table 1 and the smallest molecular cross-section (∼40 Å^2) calculated by adopting the above-described model, indicates that only 3% of the photons impinging the sample are absorbed by the layer molecules, which essentially stand up onto the ITO/glass electrode. From the previous considerations a coverage of 3.5×10^{-10} mol cm^{-2} is derived. Thus, the optical results substantially confirm the CV analysis.

The grafting of UT3 occurs similarly. CV shows an irreversible oxidation process as a broad response at the same potential as for T3 involving the same charge. The UV−vis spectrum shows a peak at 410 nm with an absorbance of 20×10^{-3}. Because the extinction coefficient is practically the same as that for T3, the coverage is only slightly lower (2.5×10^{-10} mol cm^{-2}). In view of the similar molecular cross-section (∼36 Å^2), the different coverage should be interpreted in terms of different packing arrangements, as found in T6 and UT6 films.[23,24]

A quite different situation occurs for T6 and T8, which are linear molecules longer than T3 and with larger extinction coefficients (see Table 1). Unexpectedly, they show absorbances comparable with that of T3. Indeed the UV−vis spectrum of attached T6 shows a maximum at 455 nm with absorbance of 30×10^{-3}, whereas the T8 layer displays an absorbance of 25×10^{-3} at 475 nm.

On the basis of the model considerations made above, and from the increased extinction coefficients and cross-sections, one could infer absorbances larger than those measured. The experimental result clearly maps a lower coverage due to an increase of the tilting angle formed by the molecular axis and the normal to the electrode plane. A less ordered aggregation in each layer is the result.

These observations are in agreement with the CV coulometric data. The voltammogram of attached T6 (Figure 1b) and T8 (Figure 1c) shows the two one-electron reversible oxidation processes as a broad twin response at $E° = 0.65$ and 0.90 V for the former and at $E° = 0.30$ and 0.60 V for the latter. The reversible charge is ca. 30 μC cm^{-2} for both, compatible with a monolayer (ca. 1.5×10^{-10} mol cm^{-2}) less dense than that for T3.

The subsequent sequential condensations, described in the following sections, are affected by this basement arrangement, i.e., they proceed with a relative order for T3 in contrast with a progressive disorder passing to T6 and T8.

3.3. Sequential Condensation of T3 and UT3. Sequential azomethine condensation of T3/DAF, monitored by UV−vis spectroscopy (Figure 2), shows a progressive increase of the absorbance accompanied by a bathochromic shift from 400 in the ATS/T3 layer to 460 nm in the ATS/T3/(DAF/T3)$_4$ sequence (Figure 3). The absorbance increase for each T3/DAF step is 20×10^{-3}. The same results are obtained with DAB.

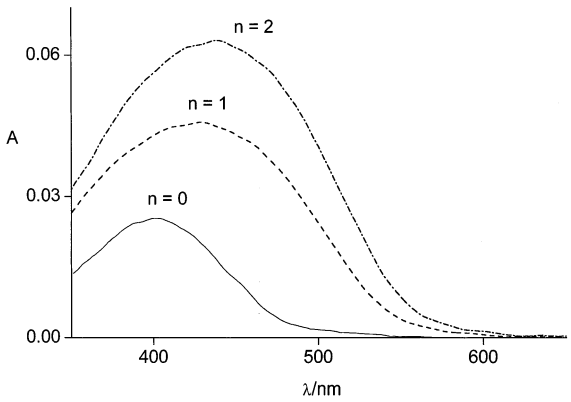

Figure 2. UV−Vis spectra of T3/(DAF/T3)$_n$ sequences (n = 0, 1, and 2) on ATS-primed ITO/glass.

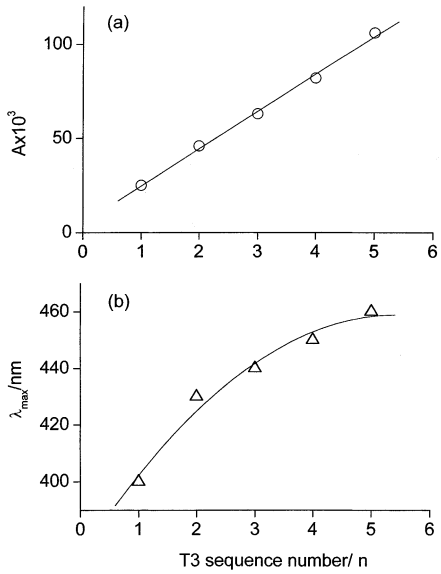

Figure 3. Progressive UV−vis (a) absorbance and (b) maximum absorption of T3/(DAF/T3)$_n$ sequence (n = 0−5) on ATS-primed ITO/glass.

Comparison of this oligomer chain with the homologous bulk polyazomethine oligomer from T3 and DAB (degree of polymerization, DP = 9), which displays a maximum absorption at 470 nm (2.64 eV),[14] confirms the regular occurrence of the condensation toward optical saturation.

The CV of the ATS/T3/(DAF/T3)$_4$ sequence shows a partially reversible oxidation at $E°_{ox} = 0.80$ V and a reversible reduction at $E°_{red} = -1.90$ V. Full oxidation requires an irreversible charge of ca. 400 μC cm^{-2}, in fair agreement with a full (two-electron) oxidation of the oligothiophene components of the sequence.

In a step-by-step CV analysis of a ATS/T3/(DAF/T3)$_3$ sequence (Figure 4) it was found that the current response (and the related irreversible charge) increases linearly with the amount of the T3 component. The response is the simple oxidation peak at ca. 0.8 V if the terminal moiety is T3, whereas when DAF is the end of the sequence the CV shows an additional oxidation process as a shoulder at 0.3 V attributable to the

(22) Lakowicz J. R. *Principle of Fluorescence Spectroscopy*; Kluwer Academic: New York, 1999;, p 56.

(23) Destri, S.; Ferro, D. R.; Khotina, I. A.; Porzio, W.; Farina, A. *Macromol. Chem. Phys.* **1998**, *199*, 1973.

(24) Porzio, W.; Destri, S.; Mascherpa, M.; Brückner, S. *Acta Polym.* **1993,** *44*, 266.

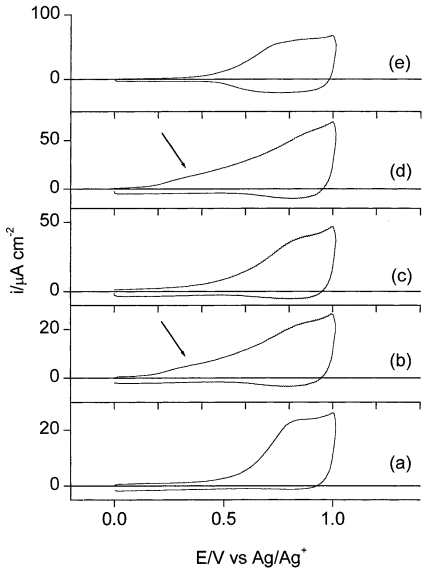

Figure 4. Cyclic voltammograms of ATS/T3/$(DAF/T3)_2$ progression in acetonitrile + 0.1 M Bu_4NClO_4. Scan rate: 0.1 Vs^{-1}. From bottom: (a) ATS/T3; (b) ATS/T3/DAF; (c) ATS/T3/DAF/T3; (d) ATS/$(T3/DAF)_2$; (e) ATS/$(T3/DAF)_2$/T3.

aromatic amine terminal moiety. The alternate presence of this DAF marker further confirms the regularity of the sequential condensation.

Sequential azomethine condensation using UT3 is similar to that observed with T3, being characterized by a progressive increase of the absorbance accompanied by a bathochromic shift from 410 nm in the spectrum of ATS/UT3 layer to 440 nm in the spectrum of ATS/UT3/$(DAF/UT3)_4$ sequence. The absorbance increase for each UT3/DAF step is also in this case 20×10^{-3}.

Though we particularly investigated sequences up to the 5th terthiophene step, the sequential deposition can be performed further. However, it was observed that in some instances a major increase of absorbance is obtained. In such cases washing with hot chloroform dissolves yellow oligomers, leading the absorbance back to the linearly extrapolated value. For this reason we argue that in thicker layers occasional trapping of precursors initiates polymer growth at sites unconnected with the electrode surface. Thus, very careful washing procedures are recommended in order to avoid the presence of only physisorbed starting molecules and oligomers.[8]

Tetrahexylsexithiophene molecule, quite similar to T6, can be vacuum-deposited into ordered ultrathin films (5 nm), as evidenced by XRD investigations.[25] In contrast, XRD measurements in Bragg−Brentano geometry of the brush-electrodes here reported do not show any coherent diffraction effect, indicating no order of the oligomers, at least along the direction normal to the ITO substrate.

3.4. Electrochemistry of Bulk Poly(T3-DAB). To compare the CV responses of T3/DAF sequences with those of the relevant oligomers, we performed electrochemistry on the chemically produced bulk poly(T3-DAB) which is in fact a nonamer.[14] This oligomer has been investigated as films cast from chloroform solution. The CV in acetonitrile + 0.1 M Bu_4NClO_4 shows a partially reversible oxidation process ($E°_{ox} = 0.76$ V) and a fully reversible reduction process ($E°_{red} = -1.90$ V) involving approximately the same charge. The electrochemical gap ($\Delta E° = E°_{ox} - E°_{red}$) is 2.75 V, in good agreement with the optical gap (2.65 eV). More important is the correspondence of the oligomer $E°$ values with those of the ATS/T3/$(DAF/T3)_4$ sequence so that the similarity of the brush-electrode sequence and of the oligomer is once more established.

The charge involved in the reversible reduction of the oligomer and related to the mass corresponds to one electron per repeat unit. Given the comparable charge used in the oxidation process it appears that the oligomer is symmetrically oxidized and reduced.

3.5. Sequential Condensation of T6. Sequential azomethine condensation with DAF or DAB proceeds also in the case of T6 with a progressive increase of the absorbance (ca 15×10^{-3} per T6 step) accompanied by a bathochromic shift from 455 nm in the ATS/T6 layer to 490 nm in the formal ATS/T6/$(DAF/T6)_4$ sequence. The absorbance of the initial T6 layer (30×10^{-3}) is appreciably higher (twice) than the progressive increase, which is accounted for considering the disorder of the layer, i.e., molecules physisorbed only and/or lying down onto the substrate (see the modeling considerations above). Furthermore, at higher levels (more than 5 formal T6 units) the progression slows down and stops.

This behavior was confirmed by coulometry. The voltammogram of the formal ATS/T6/$(DAF/T6)_4$ sequence shows the two one-electron reversible oxidation processes of T6 negatively shifted to $E° = 0.50$ and 0.70 V. This result supports the increased conjugation indicated by the optical shift. However, the amount of reversible charge involved in the sequence is only 90 $\mu C\ cm^{-2}$ so that the formal ATS/T6/$(DAF/T6)_4$ is in fact ATS/T6/$(DAF/T6)_2$ and the suggestion that lower amounts are attached in subsequent layering is confirmed. The effective ATS/T6/$(DAF/T6)_2$ sequence is reduced with partial reversibly at $E° = -2.05$ V.

3.6. Attempted Sequential Condensation of T8. In this case sequential azomethine condensation proceeds with high difficulty. In a formal ATS/T8/$(DAF/T8)_3$ sequence the absorbance of the initial T8 layer increases slightly (from 25 to 40×10^{-3} only) and the maximum absorption shifts from 475 to 485 nm only.

The voltammogram of such sequence shows the two one-electron reversible oxidation processes at the same $E°$ of the monolayer with only a modest (ca 50%) increase of the reversible charge. Therefore, much lower amounts of T8 are attached in the steps following the first one.

To account for this result the disorder already considered for the T6 layer is envisaged also for the T8 layer basis. The failed sequential growth is also accounted for in this case by detachment of fragments in the layering procedure. In fact, multiple subsequent DAF treatments of the initially reacted T8 on ATS showed that each treatment decreases the T8 coverage by ca. 50%. The same treatment leaves the ATS/T3 and ATS/T6 monolayers perfectly unchanged. The action of DAF in this degradation process, confirmed with tests performed in its absence, is the detachment of the T8 moieties by reaction of the amine with the imine groups present at

(25) Botta, C.; Destri, S.; Porzio, W.; Sassella, A.; Borghesi, A.; Tubino, R. *Opt. Mater.* **1999**, *12*, 301.

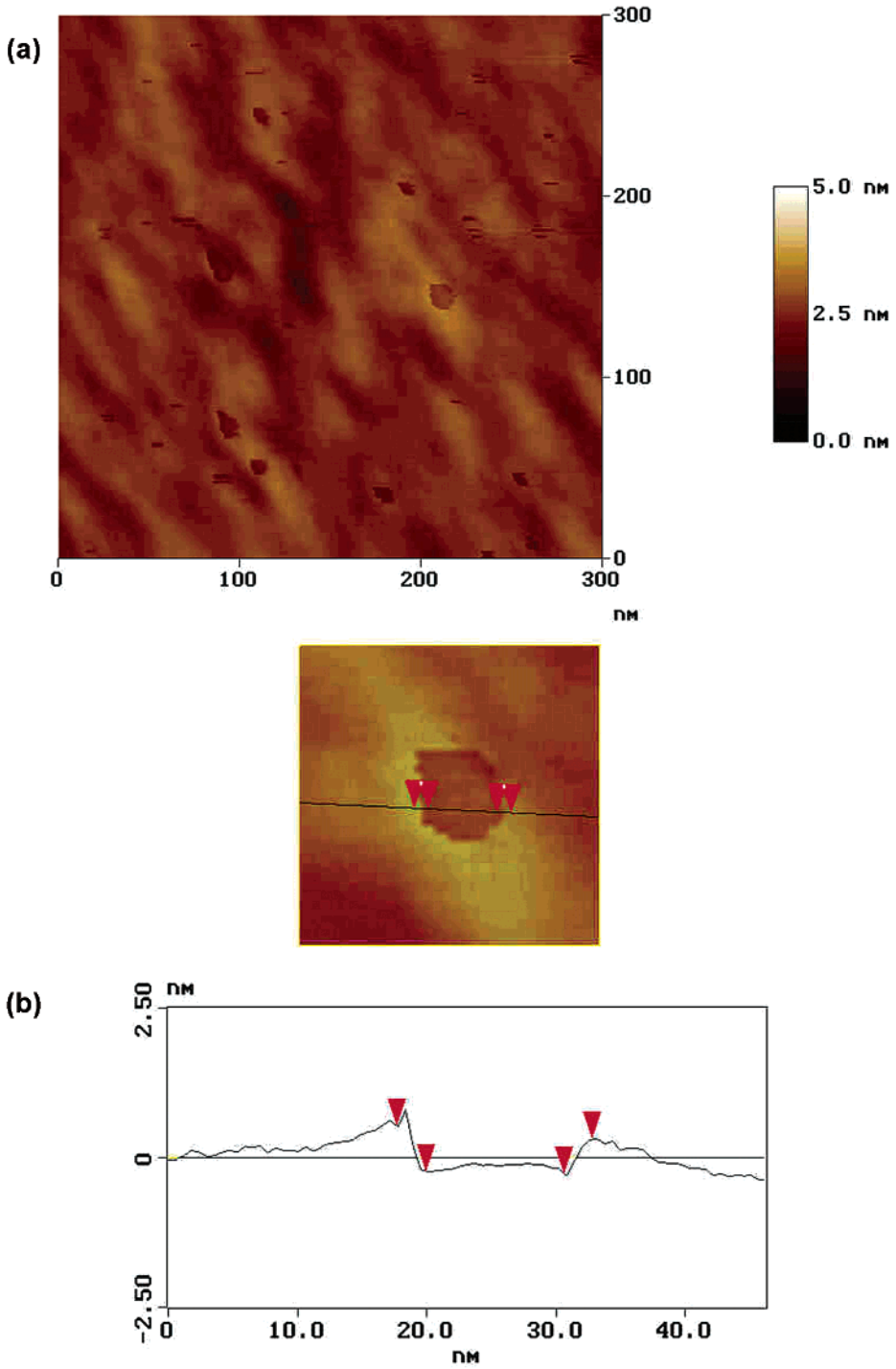

Figure 5. AFM (a) general micrograph and (b) detail micrograph + profile for a ATS/T3/$(DAF/T3)_2$ sequence.

the surface. A decreased reactivity of the longer chains is expected on the basis of the increased conjugation of the carbonyl and amine terminal moieties. Thus, condensation of longer oligomers is unfavored, whereas on the contrary their hydrolysis or substitution is eased.

A final likely explanation of the failed (for T8) or limited (for T6) sequential growth is the occurrence of two-end condensation of the longer oligomers (T8 and to a lesser extent T6) with the amine sites of the ATS-primed surface. The T3 oligomers are short enough to stand up and produce only one-end attachment, whereas the length of T8 (ca. 3.3 nm) favors the molecule lying on the surface as it matches the distance of two amine sites placed in a reliable pseudohexagonal arrangement of ca. 0.7-nm radius. With T6 an intermediate situation occurs, and the multiple layering, which is 100% with T3 and almost zero with T8, is ca. 50%.

3.7. Atomic Force Microscopy Analysis of Sequences. Because the ITO side of the ITO/glass electrode is not suitable for this type of analysis given its high roughness (5 nm rms), we have imaged and compared the surfaces of glass substrates as such, ATS-primed, monolayered at the ATS-primed surface, and sequenced. Topographic images of $0.3 \times 0.3\ \mu m^2$ dimension were obtained and the relevant profiles were measured. The blank substrate is very flat with low slopes ca. 0.1 nm high and 100 nm apart. The hills increase in height to a rms roughness of 0.5 nm when

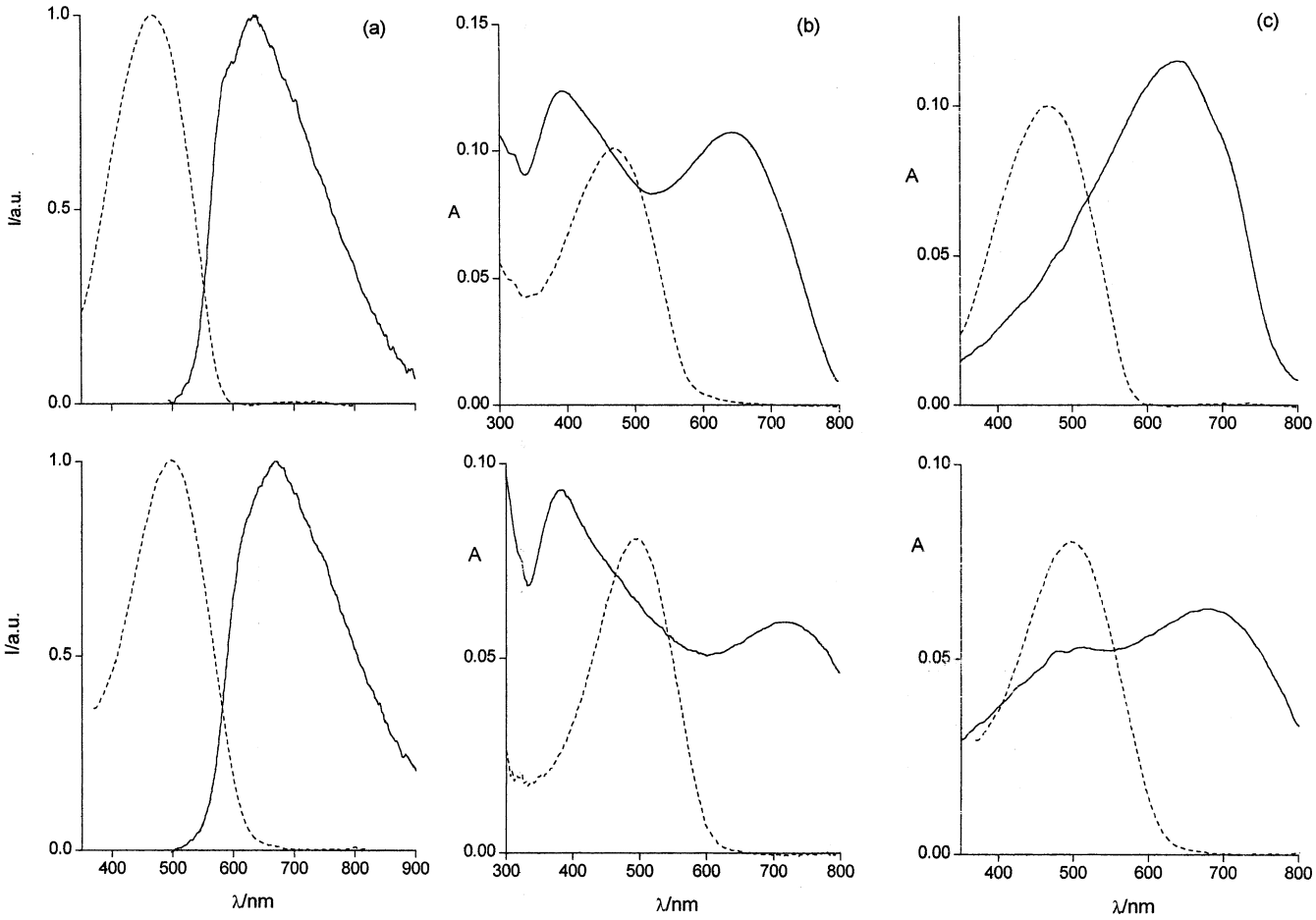

Figure 6. (a) Absorption (- - - -) and photoluminescence (——) spectra; (b) UV−vis spectra before (- - - -) and after (——) I_2-doping; (c) UV−vis spectra before (- - - -) and after (——) H^+-doping of ATS/T3/$(DAF/T3)_4$ (upper) and ATS/T6/$(DAF/T6)_2$ (lower) sequences on ITO/glass.

the substrate is reacted with ATS, but morphological changes are minor. The adsorption of all the oligothiophenes onto the ATS-primed substrate results in a surface morphology similar to that seen for the primer layer (Figure 5a). An interesting feature is that the same roughness (0.5 nm) is kept at the higher sequences for all the oligothiophenes. This result is unusual because in polymer multilayering, roughness increases progressively as multilayering proceeds.[26]

However, this is a positive result for a regular multilayering. In contrast to this, in the case of T3 the deposition shows some defects (more frequent at the early layering steps) appearing as dark dots in the micrograph (Figure 5a). It appears that the layers contain nanoscale domains, typically 10 nm in diameter, separated by domain walls. These defects are attributable to lost adsorbates or failed condensation. The profile evidences at their edges sharp height drops of ca. 1 nm, a distance corresponding roughly to the calculated monomer length. For instance, in the case of a ATS/T3/$(DAF/T3)_2$ sequence the height drop of 0.8 nm (Figure 5b) is comparable with the monomer length of 1.3 nm, the lower value mapping the tilting of the molecular brushes from the surface normal (see above). Similar defects were observed by STM in self-assembled monolayers of alkanethiols on gold.[27] As the sequence proceeds, the density of these defects decreases, disappearing at the ATS/T3/$(DAF/T3)_5$ sequence, as for a progressive "healing" process.

3.8. Photoluminescence of Sequences. The photoluminescence (PL) properties of our sequences were investigated, in view of a possible application in LEDs as a new method to directly prepare the polymer onto the ITO electrode. The PL of the ATS/T3/$(DAF/T3)_5$ and ATS/T6/$(DAF/T6)_2$ sequences (Figure 6a) display maxima at 640 and 670 nm respectively, i.e., with a 170-nm red shift from the absorption maxima. It is noteworthy that the response of the T3 sequence matches that reported for bulk poly(T3-DAB) in solution,[14] thus providing further evidence of their quite similar compositions.

3.9. I_2- and H^+-Doping of Sequences. ATS/T3/$(DAF/T3)_4$ and ATS/T6/$(DAF/T6)_2$ sequences were iodine-doped to test their ability to become conductive, a useful property to perform as conducting-wire brush-electrodes. Such doping was observed to occur even in simple polyazomethines giving conductivities of ca. 1 S cm^{-1}.[28] Also, their ability to coordinate protons, which was shown to cause marked bathochromic shifts in other polyazomethines,[13] was checked.

(26) Lvov, Y.; Essler, F.; Decher, G. *J. Phys. Chem.* **1993**, *97*, 13773.

(27) Edinger, K.; Golzhauser, A.; Demota, K.; Woll, Ch.; Grunze, M. *Langmuir* **1993**, *9*, 4.

(28) Hauer, C. R.; King, G. S.; McCool, E. L.; Euler, W. B.; Ferrara, J. D.; Youngs, W. J. *J. Am. Chem. Soc.* **1987**, *109*, 5760.

I_2-doping was performed by exposure to iodine vapors for 1 h. The treatment changes the color of the multilayers to blue (Figure 6b). The reversibility of the doping has been checked by dedoping with hydrazine which fully regenerates the pristine material, though hot air is enough to practically eliminate the dopant. The appearance upon doping of an absorption in the low-energy range (at 645 and 715 nm for the T3 and T6 sequences respectively) is characteristic of doped oligothiophenes, whereas the strong maximum at 380 nm is peculiar of I_2-doped polythiophene.[29]

Ionochromic effects of protons are known with polyazomethines and attributed to the ion-coordination-induced coplanarization of the polymer subunits.[13] In these materials the optical transitions show a strong bathochromic shift of the band upon protonation or quaternization of the lone pair of the nitrogen atoms. Protonation with 0.1 M $HClO_4$ in acetonitrile produces a bathochromic shift of the UV−vis maxima from 470 to 640 nm in the T3 sequence and from 500 to 680 nm in the T6 sequence (Figure 6c). Deprotonation and protonation steps are fully reversible as washing in acetonitrile regenerates the original spectrum, probably because of the proton scavenging action of the water content of the medium.

(29) Cao, Y.; Guo, D.; Pang, M.; Quian, R. *Synth. Met.* **1987**, *18*, 189.

4. Conclusions

The sequential condensation of aldehyde end-capped oligothiophenes with *p*-diaminobiphenyle or *p*-diaminofluorene on 3-aminopropyltrimethoxysilane-primed ITO/glass was obtained with success from terthiophene T3, but only partially from sexithiophene T6, whereas it was completely unsuccessful with octathiophene T8. Whereas the first oligothiophene layers produced from T3 on the primed-ITO are densely packed, those produced from T6 and T8 are less dense and more disordered with consequent partial (T6) or total (T8) blocking of the sequential growth.

Typical brush-electrodes constituted by T3 and T6 condensed sequences are fluorescent and display ionochromic properties. Particularly interesting for their possible application as nanowire electrodes is their reversible iodine-doping to a conducting state.

Acknowledgment. We thank S. Sitran (CNR) for his technical assistance and Dr. C. Botta (CNR) for emission measurements.

CM020619V